

EgoTV : Egocentric Task Verification from Natural Language Task Descriptions

Rishi Hazra¹ Brian Chen² Akshara Rai² Nitin Kamra² Ruta Desai²

¹Örebro University, ²Meta

rishi.hazra@oru.se, {bc2754, nitinkamra}@meta.com, {akshararai, rutadesai}@fb.com,

Abstract


To enable progress towards egocentric agents capable of understanding everyday tasks specified in natural language, we propose a benchmark and a synthetic dataset called Egocentric Task Verification (EgoTV). EgoTV contains multi-step tasks with multiple sub-task decompositions, state changes, object interactions, and sub-task ordering constraints, in addition to abstracted task descriptions that contain only partial details about ways to accomplish a task. We also propose a novel Neuro-Symbolic Grounding (NSG) approach to enable the causal, temporal, and compositional reasoning of such tasks. We demonstrate NSG’s capability towards task tracking and verification on our EgoTV dataset and a real-world dataset derived from CrossTask [81] (CTV). Our contributions include the release of the EgoTV and CTV datasets, and the NSG model for future research on egocentric assistive agents.

1. Introduction

Inspired by recent progress in visual systems [1, 64], we consider an assistive egocentric agent capable of reasoning about daily activities. When invoked via natural language commands, for e.g., while baking a cake, the agent understands the steps involved in baking, tracks progress through the various stages of the task, detects and proactively prevents mistakes by making suggestions. Such an agent would empower users to learn new skills and accomplish tasks efficiently.

Developing such an egocentric agent capable of tracking and verifying everyday tasks based on their natural language specification is challenging for multiple reasons. First, such an agent must reason about various ways of doing a *multi-step* task specified in natural language. This entails decomposing the task into relevant actions, state changes, object interactions as well as any necessary causal and temporal relationships between these entities. Secondly, the agent must ground these entities in egocentric observations to track progress and detect mistakes. Lastly,

to truly be useful, such an agent must support tracking and verification for a combination of tasks and, ideally, even unseen tasks. These three challenges – causal and temporal reasoning about task structure from natural language, visual grounding of sub-tasks, and compositional generalization – form the core goals of our work.

As our first contribution, we propose a benchmark – **Egocentric Task Verification** (EgoTV ) – and a corresponding dataset in the AI2-THOR [30] simulator. Given a natural language (NL) task description and a corresponding egocentric video of an agent, the goal of EgoTV is to verify whether the task was successfully completed in the video or not. EgoTV contains multi-step tasks with *ordering* constraints on the steps and *abstracted* NL task descriptions with omitted low-level task details inspired by the needs of real-world assistants. We also provide splits of the dataset focused on different generalization aspects, e.g., unseen visual contexts, compositions of steps, and tasks (see Figure 1).

Our second contribution is a novel approach for order-aware visual grounding – **Neuro-Symbolic Grounding** (NSG), capable of compositional reasoning and generalizing to unseen tasks owing to its ability to leverage abstract NL descriptions and compositional structure of tasks (task decomposition, ordering). In contrast, state-of-the-art vision-language models [75, 49, 37, 5] struggle to ground NL descriptions in egocentric videos, and do not generalize to unseen tasks. NSG outperforms these models by **33.8%** on compositional generalization and **32.8%** on abstractly described task verification. Finally, to evaluate NSG on real-world data, we instantiate EgoTV on the CrossTask [81] instructional video dataset. We find that it also outperforms state-of-the-art models at task verification on CrossTask. We hope that the EgoTV benchmark and dataset will enable future research on egocentric agents capable of aiding in everyday tasks.

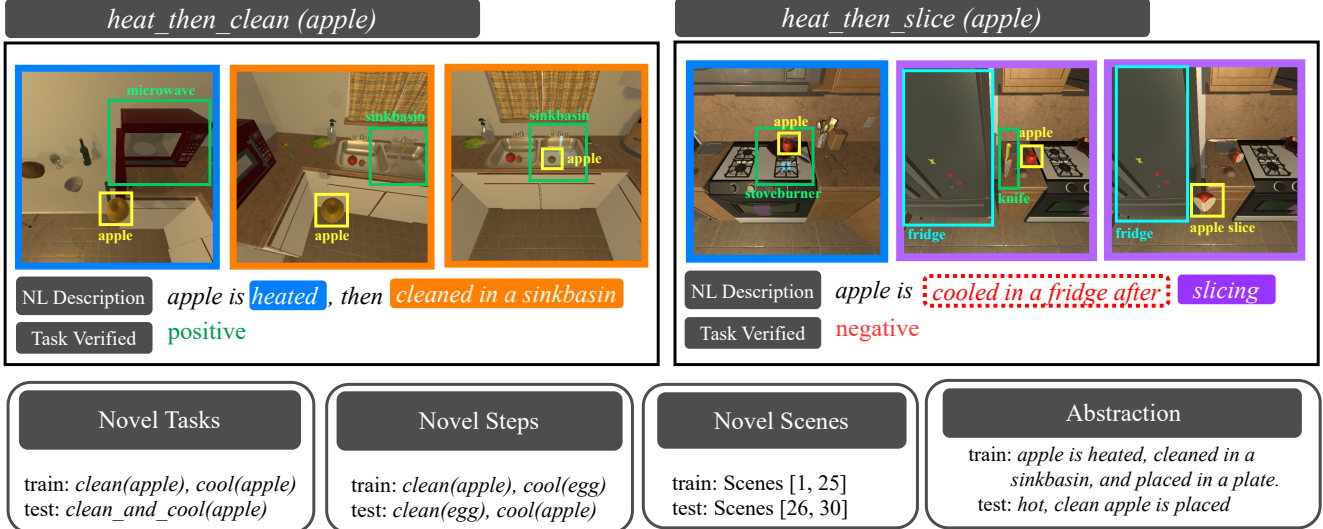


Figure 1. **EgoTV benchmark.** A positive example [Left] and a negative example [Right] from the train set along with illustrative examples from the test splits [Bottom] of EgoTV are shown. The test splits are focused on generalization to novel compositions of tasks, unseen sub-tasks or steps and scenes, and abstraction in NL task descriptions. The bounding boxes are solely for demonstration purposes and are not used during training/inference.

2. Related Work

Video-based Task Understanding. Understanding tasks from videos has been a long-standing theme in vision research with focus on recognizing activities [57, 12], human-object interactions [26, 18], and object state changes [59, 15] using egocentric or exocentric videos. But apart from recognizing actions, objects, and state changes, task verification also requires understanding temporal orderings between them. Our work is, therefore, closer to research on understanding instructional tasks [81, 61], which require reasoning about multiple, ordered steps. Prior works focus on either learning the order of steps [6, 38, 25, 42] or use step-ordering as a supervisory signal for learning step-representations or step-segmentation [81, 55]. Instead, we are focused on video-based order verification of steps described in NL, akin to [48].

Temporal Video Grounding. Our EgoTV benchmark is also closely related to the problem of Temporal Video Grounding (TVG) [2, 21, 51, 59]. However, prior work on TVG predominantly focuses on localizing a single action in the video [58, 28]. In contrast, EgoTV requires localizing multiple actions, wherein actions could have partial ordering, i.e., actions could have more than one valid ordering amongst them.

Vision-Language Benchmarks. Various benchmark tasks have been proposed for enabling models that can reason across video and language modalities (see Table 1). Examples include video question answering [73, 68, 19, 22, 67, 32, 62, 17], video-based entailment [39], and embodied task completion [56, 46, 60]. However, these benchmarks fo-

cus on individual specific aspects of multimodal reasoning, e.g., compositional reasoning (AGQA [19], ActivityNet-QA [22], TVQA [32], and CATER [17]) or causal reasoning (NExT-QA [68], CoPhy [7], Causal-VidQA [34], EgoTaskQA[27], and VIOLIN [39]). In comparison, EgoTV focuses on both causal and compositional reasoning and further requires visual grounding of both objects and actions from text, similar to STAR [67] and CLEVRER [73], albeit in egocentric settings. Unlike embodied instruction following (ALFRED [56], TEACH [46]), which requires interpreting grounded task instructions for task execution, EgoTV focuses on task verification in egocentric videos from instruction-like descriptions. Akin to NLP *Entailment* problem [11, 69], it can also be viewed as a video-based entailment problem – where a given “premise” (video) is validated by a “hypothesis” (task description).

Vision-Language Models. Vision-Language Models (VLMs) [49, 37, 40, 33, 75] pre-trained on large-scale image-text or video-language narration pairs have demonstrated enhanced performance on certain compositional [35] and causal [59] tasks. However, they generally struggle to handle compositionality and order sensitivity [76, 63]. Instead, NSG explicitly targets order awareness and compositionality for generalization in task verification using neuro-symbolic reasoning.

Neuro-symbolic Models. Neuro-symbolic models combine feature extraction through deep learning with symbolic reasoning [53, 67] to capture compositional substructures. These models either reason on static images to recognize object attributes and relations (NS-CL [41], NS-VQA [74], CLOSURE [8], and ∇ -FOL [4]), or on videos to recog-


	Reasoning			Dataset Characteristics		
	compositional	causal	temporal	egocentric	real-world	diagnostic tools
CLEVRER [73]	✓	✓	✓	✗	✗	✓
Next-QA [68]	✗	✓	✓	✗	✓	✓
ActivityNet-QA [22]	✗	✗	✓	✗	✓	✗
STAR [67]	✓	✓	✓	✗	✓	✓
Causal-VidQA [34]	✗	✓	✗	✗	✓	✓
EPIC-KITCHENS [12]	✓	✓	✗	✓	✓	✓
Ego-4D [18]	✗	✓	✗	✓	✓	✓
VIOLIN [39]	✗	✓	✗	✗	✓	✗
Cross-Task [81]	✓	✗	✓	✗	✓	✗
EgoTV 	✓	✓	✓	✓	✗	✓

Table 1. **EgoTV vs. existing video-language datasets.** EgoTV benchmark enables systematic investigation (diagnostics) on compositional, causal (e.g., effect of actions), and temporal (e.g., action ordering) reasoning in egocentric settings. Table 4 in Appendix provides a more comprehensive comparison.

nize spatio-temporal and causal relations (NS-DR [73] and DCL [10]). We extend this to tracking multi-step actions.

3. EgoTV Benchmark and Dataset

We present the *Egocentric Task Verification* (EgoTV) benchmark and dataset. To enable task tracking and verification for real-world egocentric agents, EgoTV contains: 1) *multi-step* tasks with *ordering constraints* to capture the causal and temporal nature of everyday tasks, 2) *multimodality* – language in addition to the egocentric video to allow language-based human-agent interaction. EgoTV also provides data for a systematic study of generalization in task verification (see Table 1). To this end, we create the EgoTV dataset using a photo-realistic simulator AI2-THOR [30] – as a rich testbed for future research on generalizable agents for task tracking and verification. We also provide a reduced study of EgoTV on real-world data using the CrossTask dataset [81].

3.1. Definitions

Benchmark. The objective is to determine if a task described in natural language has been correctly executed by the agent in a given egocentric video.

Tasks. Each task in EgoTV consists of multiple *partially-ordered sub-tasks* or steps. A sub-task corresponds to a single object interaction via one of the six actions: *heat*, *clean*, *slice*, *cool*, *place*, *pick*, and is parameterized by a *target* object of interaction¹. By using the “actionable” properties of objects in AI2-THOR [30], we ensure that the sub-tasks are parameterized with appropriate target objects in EgoTV, e.g., *heat(book)* will never occur.

¹Except the *place* sub-task, which is additionally parameterized by a *receptacle* object, we currently limit our EgoTV dataset to sub-tasks involving only a single target object.

Real-world tasks consist of sub-tasks with ordering constraints, either due to physical restrictions (e.g., picking up a knife before slicing) or task semantics (e.g., slicing vegetables before frying). We allow EgoTV tasks to be partially ordered, with some steps following strict ordering, e.g. *pick* sub-task happens before *place* sub-task, while others are order-independent. The ordering constraints between sub-tasks are captured in the task description using specifiers such as *and*, *then*, and *before/after*. For ease of description, we will refer to a task in the paper using $\langle \text{sub-task} \rangle - \langle \text{ordering-specifier} \rangle (\text{object})$ notation, irrespective of the actual task description. An example task from EgoTV: *heat_then_clean(apple)* is shown in Fig. 1 with its NL description: “apple is heated, then cleaned in a sinkbasin”. The task consists of two ordered sub-tasks: *heat* \rightarrow *clean* on *target*: *apple*.

3.2. Dataset

As shown in Fig. 1, EgoTV dataset consists of (task description, video) pairs with positive or negative task verification labels. By combining the six sub-tasks *heat*, *clean*, *slice*, *cool*, *put*, *pick* with different ordering constraints, we create 82 tasks for EgoTV (see Appendix 7.3 for an exhaustive list). Tasks are instantiated with 130 target objects (excluding visual variations in shape, texture, and color) and 24 receptacle objects, totaling 1038 task-object combinations. These are performed in 30 different kitchen scenes. We also provide comprehensive annotations for each video, including frame-by-frame breakdowns for sub-tasks, object bounding boxes, and object state information (e.g., *hot*, *cold*, etc.) to facilitate future research.

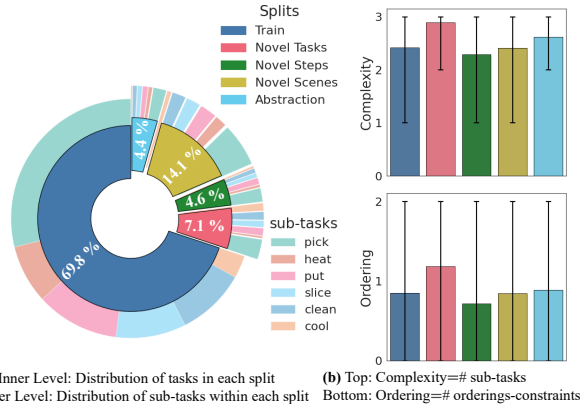


Figure 2. **EgoTV dataset.** Sub-tasks and tasks, including their difficulty measures (Sec: 3.2.2) are shown per split. Novel Scenes have more tasks since all the train tasks are repeated in unseen scenes. Likewise, complexity and ordering are higher in Novel Tasks due to the addition of unseen sub-tasks.

3.2.1 Generation

Task-video Generation. We generate the videos in our dataset by leveraging the ALFRED setup [56]. ALFRED allows us to specify the EgoTV tasks using Planning Domain Definition Language (PDDL) and then to generate plans for achieving these tasks using the Metric-FF planner [24]. We execute these plans using the AI2-THOR simulator and obtain their corresponding videos. Further details on encoding tasks using PDDL and planning are in Appendix 7.1.

Task-description Generation. We convert the plans generated for each task into positive and negative task descriptions using templates. Appendix 7.2 provides details on the process and example templates.

3.2.2 Evaluation

Metrics. We use accuracy and F1 to measure the efficacy of models on EgoTV task verification benchmark. To capture the difficulty of tracking and verifying tasks, we introduce two measures: (1) *Complexity*: measuring the number of sub-tasks in a task, which impacts the video length and requires higher action and object grounding, and (2) *Ordering*: measuring the number of ordering constraints in a task and measures the difficulty of temporal reasoning required to track and verify tasks. We evaluate model scalability by testing on tasks with varying complexity and ordering.

Generalization. Our synthetic dataset facilitates a systematic exploration of generalization in task tracking and verification via four test splits that focus on generalization to novel steps, tasks, visual contexts/scenes, and abstract task descriptions.

- **Novel Tasks:** Unseen compositions of seen sub-tasks. For e.g., if train set is $\{clean(apple), cool(apple)\}$,

then this test split would contain tasks like: $\{clean_and_cool(apple), clean_then_cool(apple), cool_then_clean(apple)\}$.

- **Novel Steps:** Unseen compositions of sub-task actions and target objects. For e.g., if the train set is $\{clean(apple), cool(egg), clean_and_cool(tomato)\}$, then this test split would contain tasks like: $\{clean(egg), cool(apple), clean_and_cool(apple)\}$.
- **Novel Scenes:** This test split contains the same tasks as in the train set. However, the tasks are executed in unseen kitchen scenes.
- **Abstraction:** Abstract task descriptions, which lack the low-level details of the task in the descriptions. For instance, for a *heat_and_clean(apple)* task, the full task description in the train set could be “apple is heated in a microwave and cleaned in sink basin”, while the abstract task description in this split could be “apple is heated and cleaned”.

Note that all the test splits and the train set are disjoint from each other. Novel Steps split tests an EgoTV model’s ability to understand generalizable object affordances and tool usage. For instance, once a model learns the *slice* action on an apple, this split tests if the model can apply it to an orange. On the other hand, the Novel Tasks split tests the generalization of a model’s causal reasoning capabilities on unseen compositions and orderings of known sub-tasks.

3.2.3 Statistics

EgoTV dataset consists of 7,673 samples (train set: 5,363 and test set: 2,310). The split-wise division is Novel Tasks: 540, Novel Steps: 350, Novel Scenes: 1082, Abstraction: 338. The total duration of the egocentric videos in the EgoTV dataset is 168 hours, with an average video length of 84 seconds. The task descriptions consist of 9 words on average, with a total vocabulary size of 72. On average, there are 4.6 sub-tasks per task in the EgoTV dataset, and each sub-task spans approximately 14 frames. Additionally, there are 2.4 ways to verify a task. Figure 2 shows a comparison of train and test splits (more analysis in Appendix 7.3).

4. Neuro-Symbolic Grounding (NSG)

EgoTV requires visual grounding of task-relevant entities such as actions, state changes, etc. extracted from NL task descriptions for verifying tasks in videos. To enable grounding that generalizes to novel compositions of tasks and actions, we propose the Neuro-symbolic Grounding (NSG) approach. NSG consists of three modules: a) semantic parser, which converts task-relevant states from NL task descriptions into symbolic graphs, b) query encoders, which generate the probability of a node in the symbolic graph being grounded in a video segment, and c) video

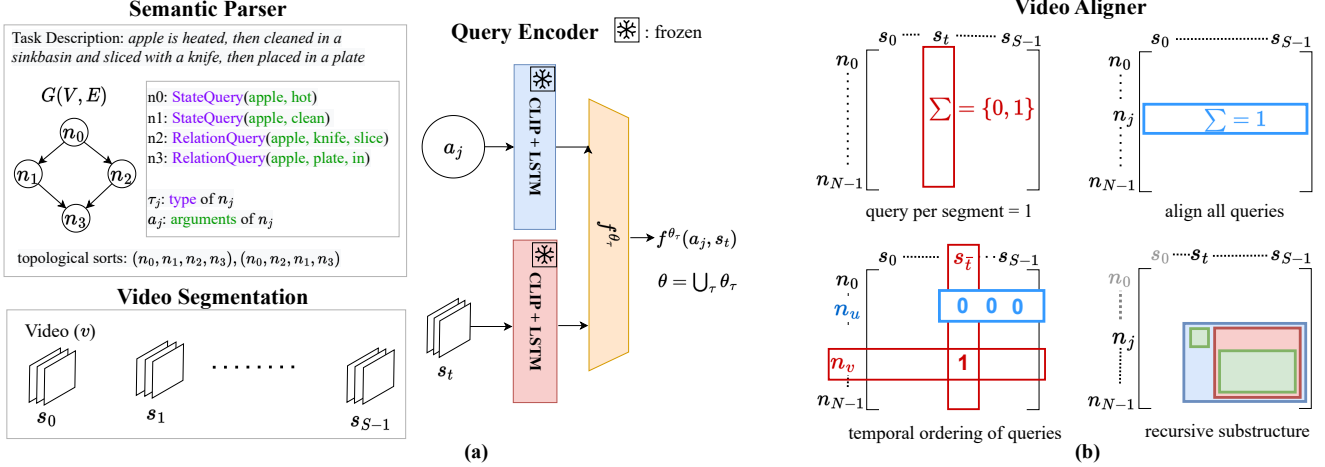


Figure 3. **NSG model** (a) semantic parser converts NL descriptions into a graph G of symbolic queries; query encoders f^{θ_τ} detect queries in individual video segments s_t ; and a video aligner aligns G with video segments by computing alignment matrix Z via a constrained optimization problem (Eq. 3). (b) The constraints (Eqs. 3a 3b 3c) and the recursive structure (Eq. 4) enabling use of DP to solve for Z . Here, the blue box denotes $F^*((n_j)_{j-1}^{N-1}, (s_t)_{t-1}^{S-1})$, the green boxes denote $\log f^\theta(a_j, s_t) + F^*((n_j)_{j+1}^{N-1}, (s_t)_{t+1}^{S-1})$, and the red box denotes $F^*((n_j)_{j-1}^{N-1}, (s_t)_{t+1}^{S-1})$.

aligner, which uses the query encoders to align these symbolic graphs with videos. NSG thus uses intermediate symbolic representations between NL task descriptions and corresponding videos to achieve compositional generalization.

4.1. Queries for Symbolic Operations

To encode tasks, NSG captures task-relevant visual and relational information in a structured manner via symbolic operators called *queries*. For instance, the task description *heat an apple* can be symbolically captured by the query: `StateQuery(apple, hot)`. Similarly, the task description *place steak on grill* can be captured by `RelationQuery(steak, grill, on)`, which represents the relation (`on`) between objects `steak` and `grill`. Queries are characterized by *types* and *arguments* and are stored in a text format. Table 6 in the appendix shows the various query types and their arguments. Different query types capture different aspects, e.g., attributes, relations, etc., thereby enabling a rich symbolic representation of everyday tasks.

4.2. Semantic Parser for Task Descriptions

The symbolic operators, i.e., queries, allow the semantic parser to represent a task’s partial-ordered steps using a symbolic graph. Specifically, the parser translates an NL task description into a graph $G(V, E)$, where a vertex $n_i \in V$ represents a query and an edge $e_{ij} : n_i \rightarrow n_j \in E$ is an ordering constraint indicating that n_i must precede n_j (Figure 3a). We experiment with two different methods to parse language descriptions of tasks to graphs – (i) finetuning language models and (ii) few-shot prompting of

language models. Appendix 9.3 describes these approaches in detail. We perform a topological sort with the graph G and generate all the possible sequences of queries consistent with the sort. For example, the topological sorting of the graph in Figure 3(a) yields two ordered sequences: $(n_0, n_1, n_2, n_3), (n_0, n_2, n_1, n_3)$. Note that this does not include all physically possible ways to complete a task, but a super-set of all possible sequences of task-relevant queries, including some infeasible sequences². However, having this super-set is useful because a task can be verified as accomplished if any sequence in this set can be ascertained to occur in the video.

4.3. Query Encoders for Grounding

Query Encoders are neural network modules that evaluate whether a query is satisfied in an input video. Specifically, a query encoder f^{θ_τ} for a query n of type τ (e.g., `StateQuery`, `RelationQuery` etc.), accepts NL arguments (a) corresponding to objects and relations in n and a video (v) to generate the probability $\mathbb{P} = f^{\theta_\tau}(a, v)$ of the desired query being true in the video. Learnable parameters corresponding to different query type encoders in an NSG model are jointly represented as $\theta = \bigcup_\tau \theta_\tau$.

Both the text arguments a of the query and the frames of the input video v are encoded using a pre-trained CLIP encoder [49]. The token-level and frame-level representations from CLIP are separately aggregated using two LSTMs [23] to obtain aggregated features for a and v , respectively.

²For instance, in Figure 3a, n_1 and n_2 are at the same topological level, but the sub-task in query n_1 could invalidate pre-conditions for n_2 . Hence, a physically plausible task requires n_2 followed by n_1 and not vice versa. Note that EgoTV does not have physically implausible tasks.

These features are then fused and passed through the neural network f^{θ_τ} to obtain the probability \mathbb{P} of the query being true in the video (see Figure 3a).

4.4. Video Aligner for Task Verification

This module of NSG must align the graph representation G of the task (generated by the semantic parser) with the video. To that end, it first segments the video, then jointly learns a) the query encoders, which detect the queries in the video segments and b) the alignment between video segments and the query sequences obtained from the topological sort on G . Such joint learning is required since the temporal locations of the queries in the video are unknown a priori requiring simultaneous detection and alignment. If the video is a positive match for the task encoded in G , at least one of the query sequences from G must temporally align perfectly with the video segments for successful task verification. Conversely, for negative matches, no query sequence from G would *completely* align with the video segments. Going forward, we use $\langle \rangle$ and $()$ to denote ordered pairs and sequences, respectively.

Video Segmentation: The video is segmented into non-overlapping segments³ with a moving window of arbitrary but fixed size k ⁴.

Joint Optimization: The objective of the optimization is to jointly learn the *alignment* Z between queries and video segments along with the *query encoders* f^θ . Given: a) the temporal sequence of S segments $(s_t)_{t=0}^{S-1}$ with each s_t spanning k image frames; and b) a sequence of N queries $(n_j)_{j=0}^{N-1}$ from the topological sort on G , the alignment Z is defined as a matrix $Z \in \{0, 1\}^{N \times S}$, where $Z_{jt} = 1$ implies that the j^{th} query n_j is aligned the video segment s_t . An example alignment with $N = 2$ and $S = 3$ is given by the matrix $Z = \begin{bmatrix} 1 & 0 & 0 \\ 0 & 0 & 1 \end{bmatrix}$, where the rows are ordered queries (n_0, n_1) , the columns are temporal segments (s_0, s_1, s_2) , and $\langle n_0, s_0 \rangle$, $\langle n_1, s_2 \rangle$ are the aligned pairs. Assuming segmentation guarantees sufficient segments for query alignment: $S \geq N$. Using Z and f^θ , the task verification probability p^θ can be defined as:

$$p^\theta = \sigma \left(\max_{Z \in \{0,1\}^{N \times S}} \frac{1}{N} \sum_{j,t} \log f^\theta(a_j, s_t) Z_{jt} \right) \quad (1)$$

Here σ is the sigmoid function, $f^\theta(a_j, s_t)$ denotes the probability of querying segment s_t using query n_j with arguments a_j (Sec. 4.3), and max operator is over the best alignment Z between N queries and S segments. We use the

³Since pretrained, off-the-shelf video segmentation models are limited to predefined action classes [14] or reliant on background frame change detection [72] and require downstream finetuning [16], we leave their integration in NSG as future work.

⁴If required, the last segment is zero-padded to k frames.

ground-truth task verification label y to compute Z and f^θ by minimizing the following loss:

$$\min_{\theta} \frac{1}{|\mathcal{D}|} \sum \mathcal{L}_{\text{BCE}}(p^\theta, y), \quad (2)$$

here $|\mathcal{D}|$ is the EgoTV dataset size and $\mathcal{L}_{\text{BCE}}(\cdot)$ is the binary cross entropy loss computed over $|\mathcal{D}|$ input, output pairs. Given the minimax nature of Eq. 2, we use a 2-step iterative optimization process: (i) find the best alignment Z between queries and segments with fixed query encoder parameters θ (optimize Eq. 1 with fixed f^θ); (ii) optimize θ using Eq. 2, given Z .

Dynamic Programming (DP)-based Alignment: Finding the best Z in Eq. 1 given θ requires iterating over combinations of N queries and S segments while respecting certain constraints. The constraints, visualized in Fig. 3b, ensure that a) no two queries are aligned to the same segment⁵ (Eq. 3a), b) all queries are accounted for in S (Eq. 3b), and c) the temporal orderings between queries in the query sequences are respected (Eq. 3c). Specifically, if query n_u precedes n_v ($n_u \rightarrow n_v$), and query n_v is paired with segment $s_{\bar{t}}$ (i.e. $Z_{v\bar{t}} = 1$), then query n_u cannot be paired with any segment that lies after $s_{\bar{t}}$ (i.e. $Z_{ut} \neq 1 \forall t \geq \bar{t}$). The resulting optimization problem for Z , given θ is:

$$\max_{Z \in \{0,1\}^{N \times S}} \sum_{j,t} \log f^\theta(a_j, s_t) Z_{jt}, \quad \text{s.t.} \quad (3)$$

$$\sum_{j=0}^{N-1} Z_{jt} \in \{0, 1\}, \quad \forall 0 \leq t \leq S-1 \quad (3a)$$

$$\sum_{t=0}^{S-1} Z_{jt} = 1, \quad \forall 0 \leq j \leq N-1 \quad (3b)$$

$$n_u \rightarrow n_v, Z_{v\bar{t}} = 1 \implies Z_{ut} \neq 1, \quad \forall t \geq \bar{t} \quad (3c)$$

Intuitively, the solution to Eq. 3 gives us the best alignment score (note, the overlap with Eq. 1). The iterations over N queries and S segments for solving Eq. 3 are underpinned by an overlapping and optimal substructure. For instance, to optimally align queries $(n_j)_{j=0}^{N-1}$ and segments $(s_t)_{t=0}^{S-1}$, one could: a) pair $\langle n_0, s_0 \rangle$ and optimally align the remaining queries and segments $(n_j)_{j=1}^{N-1}, (s_t)_{t=1}^{S-1}$; or (2) skip s_0 and still optimally align *all* queries, now with the remaining segments $(n_j)_{j=0}^{N-1}, (s_t)_{t=1}^{S-1}$ (see Fig. 3b(iv)). This recursive substructure leads to a DP solution for Eq. 3.

Let, $F^*((n_j)_{j=0}^{N-1}, (s_t)_{t=0}^{S-1})$ denote the best alignment score for queries $(n_j)_{j=0}^{N-1}$ and segments $(s_t)_{t=0}^{S-1}$ from Eq. 3. Based on the aforementioned reasoning,

⁵This ensures that the order of queries can be verified, which cannot be done when queries belong to the same segment.

$F^*((n_j)_j^{N-1}, (s_t)_t^{S-1})$ can be recursively written as:

$$F^*((n_j)_j^{N-1}, (s_t)_t^{S-1}) = \max(\log f^\theta(a_j, s_t) + F^*((n_j)_{j+1}^{N-1}, (s_t)_{t+1}^{S-1}), F^*((n_j)_j^{N-1}, (s_t)_{t+1}^{S-1})) \quad (4)$$

The base cases for the DP are: (i) $Z = \mathbb{I}$ if $N = S$; (ii) $Z_{jt} = 1 \forall t$ if $j = N - 1$. It is worth noting that the DP subproblems, together with the base cases, satisfy the constraints in Eq. 3a 3b 3c. Since the video may match any of the sequence in the super-set of query sequences (from the topological sort on G), we repeat this process of computing F^* for each sequence and select the maximum value.

Optimizing Query Encoder Parameters θ : After obtaining the best alignment Z using DP, we substitute the corresponding value of $F^*((n_j)_{j=0}^{N-1}, (s_t)_{t=0}^{S-1})$ in Eq. 1 and subsequently Eq. 2. In Eq. 2, we use single mini-batch of training examples and take one gradient-update step of the Adam optimizer for the query encoder parameters θ .

5. Experiments

We compare various state-of-the-art (SOTA) VLMs with NSG on the EgoTV benchmark (see Appendix 9.2 for NSG’s experimental training details).

5.1. SOTA VLM Baselines

We investigate 6 VLMs developed for video-language tasks requiring similar reasoning as EgoTV. Summarized in Table 2, **CLIP4Clip** [40], **CLIP Hitchhiker** [5], **CoCa** [75] use image backbones followed by temporal aggregation, while **VideoCLIP** [37], **MIL-NCE** [43], and **VIOLIN** [39] use video backbones. With the exception of CoCa, which is trained with contrastive and captioning loss, all other models are trained using contrastive loss [43]. Lastly, VideoCLIP and VIOLIN use an explicit fusion of text-vision features. For each model, we freeze all pretrained feature extractors and finetune a fully-connected probe layer, along with the temporal aggregation layers where appropriate (CLIP4Clip-LSTM, VIOLIN), using EgoTV’s train split.

Finally, to establish upper-bounds on EgoTV, we also instantiate: (1) a **Text2text model**, which constructs video captions using ground-truth labels for objects and actions, encodes the captions and task descriptions using (pre-trained) RoBERTa model [80] and measures alignment using the cosine similarity score (see Appendix 10.2), and (2) an **Oracle model**, which is trained with full supervision on sub-tasks labels and locations in addition to task verification labels.

5.2. Results

In Table 2, we show the performance of NSG vs. SOTA VLMs per split of EgoTV. (1) **Novel Tasks:** NSG significantly

outperforms other baselines due to its ability to decompose and detect sub-tasks while using DP alignment to handle temporal constraints among them. In contrast, other baselines rely on detecting the entire task under temporal constraints, which is more challenging. Further, image-based baselines outperform video-based baselines due to their ability to capture a greater degree of compositional detail through frame-level representations. (2) **Novel Steps:** NSG’s poor performance in this split could be attributed to its low precision in the *slice* sub-task (which is dominant in this split), as shown in Figure 4 [Right]. We hypothesize that since NSG only uses the aligned segments while discarding the rest, learning to utilize context from neighboring segments to capture *slice* (like picking up a knife) could be a promising future direction. (3) **Novel Scenes:** Here, NSG performs as well as the best baseline VIOLIN-ResNet. Since the tasks are identical to the train split, the success of a model is contingent on the vision encoder’s ability to accurately detect the same sub-tasks in unseen scenes. Consequently, models with an additional temporal aggregation layer (VIOLIN) finetuned on EgoTV, tend to outperform image-based models that do not have temporal aggregation (CLIP Hitchhiker) and models with frozen video features (MIL-NCE, VideoCLIP). (4) **Abstraction:** NSG significantly outperforms the baselines, primarily due to its semantic parser, which captures the underlying structure of the description and encodes the relevant concepts, such as objects and sub-tasks, to generate an (abstract) symbolic output.

5.3. Analysis of NSG

NSG learns to localize task-relevant entities without explicit supervision. Figure 4 shows the confusion matrix of `StateQuery` & `RelationQuery` outputs, which capture sub-tasks in EgoTV, with their ground truths. The high recall of NSG demonstrates its ability to successfully localize task-relevant entities, despite being trained using only task verification labels.

Effect of query types on NSG. While query types with multiple entity arguments might appear capable of modeling complex dependencies amongst entities and having more expressive power, encoding multiple entities jointly using a single encoder makes the grounding problem more challenging. Hence, in practice, we found that using a combination of `StateQuery` & `RelationQuery` types as opposed to `ActionQuery` (which encodes multiple entities using a single encoder) enabled better grounding and ultimately led to better performance in terms of F1-score (Table 3).

NSG shows consistent performance with increasing task difficulty. As seen in Figure 4, NSG’s performance is minimally affected by increase in task difficulty characterized by number of sub-tasks (complexity) and ordering constraints

Model	Visual feature	Text feature	MM Fusion	Novel Tasks	Novel Steps	Novel Scenes	Abstraction	Average
Text2text [80]		RoBERTa		64.9	65.8	66.5	64.7	65.5
CLIP Hitchhiker [5]	CLIP(I)	CLIP		43.9	66.5	72.2	13.6	49.1
CLIP4Clip mean [40]	CLIP(I)	CLIP		49.3	70.9	74.9	16.1	52.8
CLIP4Clip seqLSTM [40]	CLIP(I)	CLIP		<u>56.2</u>	73.2	74.6	17.5	55.4
CoCa [75]	Tx(I)	Tx	Y	51.5	71.6	71.9	43.5	59.6
VIOLIN-ResNet [39]	ResNet(I)	BERT	Y	47.4	80.4	85.6	42.5	64.0
MIL-NCE [43]	S3D(V)	Word2vec		30.5	69.6	73.5	24.3	49.5
VideoCLIP [37]	Tx(V)	Tx	Y	29.3	67.6	77.9	25.6	50.1
VIOLIN-I3D [39]	I3D(V)	BERT	Y	45.6	<u>79.7</u>	83.9	<u>47.6</u>	64.2
NSG (ours)	CLIP(I)	CLIP	Y	90.0	64.7	<u>84.9</u>	80.4	80.0
Oracle Model	CLIP(I)	CLIP	Y	95.0	96.7	97.6	97.2	96.6

Table 2. **Comparison of baselines with NSG on different data splits using F1-score.** MM fusion indicates multimodal fusion of vision and text features. Tx indicates the Transformer as feature extractor with image (I) and video (V) backbones. Video backbone models are highlighted in gray. Underline indicates second-best performance.

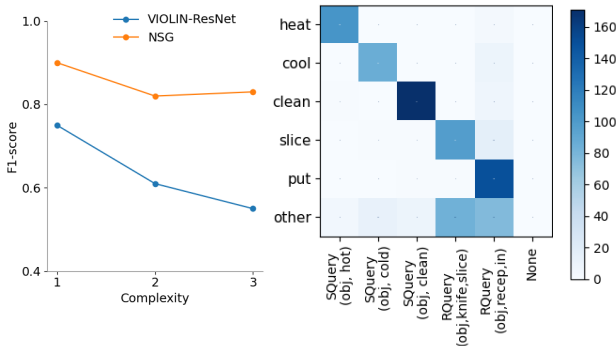


Figure 4. [Left] F1-score of NSG vs. best-performing baseline for EgoTV tasks with varying complexity averaged over all splits (Appendix 9.5 shows performance with varying ordering). [Right] Confusion Matrix for NSG Queries on validation split (SQuery: StateQuery, RQuery: RelationQuery). See Appendix 9.5 for results on all splits.

(Sec. 3.2.2) unlike the best-performing baseline (VIOLIN-ResNet).

NSG is robust to segmentation window size The effect of k on NSG is minimal (Appendix 9.5).

NSG also enables task verification on real-world data. We leverage an existing instructional video dataset CrossTask [81] to create the CrossTask Verification (CTV) dataset (see Appendix 8). NSG still outperforms all competitive baselines on CTV significantly with F1-score (NSG: **76.3**, CoCa: 70.9, VideoCLIP: 49.7, VIOLIN 34.7), demonstrating its causal and compositional reasoning capabilities in real-world applications (see Appendix 9.5 for details).

Limitations of NSG. NSG also has certain limitations: (1) It does not consider multiple simultaneous actions like “picking an apple while closing the refrigerator door”, and (2) The assumption of equal-length video segments

NSG	Novel Tasks	Novel Steps	Novel Scenes	Abstract.
Action	78.2	45.6	70.6	75.5
State+Relation	90.0	64.7	84.9	80.4

Table 3. (State + Relation) Query vs. ActionQuery

may be unsuitable for sub-tasks with a highly variable duration. We defer exploration of these limitations to future work.

6. Conclusion

To address various challenges towards the development of egocentric assistants that can track and verify the accomplishment of everyday tasks, including reasoning about causal and temporal constraints in tasks, visual grounding, and compositional generalization, we introduce Egocentric Task Verification (EgoTV), a benchmark and dataset containing partially-ordered, multi-step tasks with natural language task specifications. We also present NSG, a novel neuro-symbolic approach that enables order-aware visual grounding, and demonstrate its effectiveness on both the EgoTV dataset and a real-world dataset CTV. We hope our contributions will help in advancing research on egocentric assistants that can aid users in everyday tasks.

References

- [1] Four optics breakthroughs to power enterprise ar - magic leap. <https://www.magicleap.com/en-us/>.
- [2] Mexaction2: action detection and localization dataset. <http://mexculture.cnam.fr/xwiki/bin/view/Datasets/Mex+action+dataset>.
- [3] Zeina Abu-Aisheh, Romain Raveaux, Jean-Yves Ramel, and Patrick Martineau. An exact graph edit distance algorithm for solving pattern recognition problems. In *Proceedings*

- of the International Conference on Pattern Recognition Applications and Methods - Volume 1, ICPRAM 2015, page 271–278, Setubal, PRT, 2015. SCITEPRESS - Science and Technology Publications, Ltd.
- [4] Saeed Amizadeh, Hamid Palangi, Alex Polozov, Yichen Huang, and Kazuhito Koishida. Neuro-symbolic visual reasoning: Disentangling. In *International Conference on Machine Learning*, pages 279–290. PMLR, 2020.
 - [5] Max Bain, Arsha Nagrani, Gül Varol, and Andrew Zisserman. A clip-hitchhiker’s guide to long video retrieval. *arXiv preprint arXiv:2205.08508*, 2022.
 - [6] Siddhant Bansal, Chetan Arora, and CV Jawahar. My view is the best view: Procedure learning from egocentric videos. In *Computer Vision—ECCV 2022: 17th European Conference, Tel Aviv, Israel, October 23–27, 2022, Proceedings, Part XIII*, pages 657–675. Springer, 2022.
 - [7] Fabien Baradel, Natalia Neverova, Julien Mille, Greg Mori, and Christian Wolf. Cophy: Counterfactual learning of physical dynamics. In *International Conference on Learning Representations*, 2020.
 - [8] Ben Bogin, Sanjay Subramanian, Matt Gardner, and Jonathan Berant. Latent Compositional Representations Improve Systematic Generalization in Grounded Question Answering. *Transactions of the Association for Computational Linguistics*, 9:195–210, 03 2021.
 - [9] João Carreira and Andrew Zisserman. Quo vadis, action recognition? a new model and the kinetics dataset. In *2017 IEEE Conference on Computer Vision and Pattern Recognition (CVPR)*, pages 4724–4733, 2017.
 - [10] Zhenfang Chen, Jiayuan Mao, Jiajun Wu, Kwan-Yee Kenneth Wong, Joshua B. Tenenbaum, and Chuang Gan. Grounding physical concepts of objects and events through dynamic visual reasoning. In *International Conference on Learning Representations*, 2021.
 - [11] Ido Dagan, Oren Glickman, and Bernardo Magnini. The pascal recognising textual entailment challenge. In *Machine Learning Challenges. Evaluating Predictive Uncertainty, Visual Object Classification, and Recognising Tectual Entailment: First PASCAL Machine Learning Challenges Workshop, MLCW 2005, Southampton, UK, April 11-13, 2005, Revised Selected Papers*, pages 177–190. Springer, 2006.
 - [12] Dima Damen, Hazel Doughty, Giovanni Maria Farinella, Sanja Fidler, Antonino Furnari, Evangelos Kazakos, Davide Moltisanti, Jonathan Munro, Toby Perrett, Will Price, and Michael Wray. The epic-kitchens dataset: Collection, challenges and baselines. *IEEE Transactions on Pattern Analysis and Machine Intelligence (TPAMI)*, 43(11):4125–4141, 2021.
 - [13] Jacob Devlin, Ming-Wei Chang, Kenton Lee, and Kristina Toutanova. BERT: Pre-training of deep bidirectional transformers for language understanding. In *Proceedings of the 2019 Conference of the North American Chapter of the Association for Computational Linguistics: Human Language Technologies, Volume 1 (Long and Short Papers)*, pages 4171–4186, Minneapolis, Minnesota, June 2019. Association for Computational Linguistics.
 - [14] Victor Escorcia, Fabian Caba Heilbron, Juan Carlos Niebles, and Bernard Ghanem. Daps: Deep action proposals for action understanding. In *European conference on computer vision*, pages 768–784. Springer, 2016.
 - [15] Alireza Fathi and James M Rehg. Modeling actions through state changes. In *Proceedings of the IEEE Conference on Computer Vision and Pattern Recognition*, pages 2579–2586, 2013.
 - [16] Jialin Gao, Zhixiang Shi, Guanshuo Wang, Jiani Li, Yufeng Yuan, Shiming Ge, and Xi Zhou. Accurate temporal action proposal generation with relation-aware pyramid network. In *Proceedings of the AAAI conference on artificial intelligence*, volume 34, pages 10810–10817, 2020.
 - [17] Rohit Girdhar and Deva Ramanan. CATER: A diagnostic dataset for Compositional Actions and Temporal Reasoning. In *ICLR*, 2020.
 - [18] Kristen Grauman, Andrew Westbury, Eugene Byrne, Zachary Chavis, Antonino Furnari, Rohit Girdhar, Jackson Hamburger, Hao Jiang, Miao Liu, Xingyu Liu, Miguel Martin, Tushar Nagarajan, Ilija Radosavovic, Santhosh Kumar Ramakrishnan, Fiona Ryan, Jayant Sharma, Michael Wray, Mengmeng Xu, Eric Zhongcong Xu, Chen Zhao, Siddhant Bansal, Dhruv Batra, Vincent Cartillier, Sean Crane, Tien Do, Morrie Doulaty, Akshay Erapalli, Christoph Feichtenhofer, Adriano Fragomeni, Qichen Fu, Abrahm Gebreselasie, Cristina González, James Hillis, Xuhua Huang, Yifei Huang, Wenqi Jia, Weslie Khoo, Jáchym Kolář, Satwik Kotur, Anurag Kumar, Federico Landini, Chao Li, Yanghao Li, Zhenqiang Li, Karttikeya Mangalam, Raghava Modhugu, Jonathan Munro, Tullie Murrell, Takumi Nishiyasu, Will Price, Paola Ruiz Puentes, Merey Ramazanova, Leda Sari, Kiran Somasundaram, Audrey Southerland, Yusuke Sugano, Ruijie Tao, Minh Vo, Yuchen Wang, Xindi Wu, Takuma Yagi, Ziwei Zhao, Yunyi Zhu, Pablo Arbeláez, David Crandall, Dima Damen, Giovanni Maria Farinella, Christian Fuegen, Bernard Ghanem, Vamsi Krishna Ithapu, C. V. Jawahar, Hanbyul Joo, Kris Kitani, Haizhou Li, Richard Newcombe, Aude Oliva, Hyun Soo Park, James M. Rehg, Yoichi Sato, Jianbo Shi, Mike Zheng Shou, Antonio Torralba, Lorenzo Torresani, Mingfei Yan, and Jitendra Malik. Ego4d: Around the world in 3,000 hours of egocentric video. In *2022 IEEE/CVF Conference on Computer Vision and Pattern Recognition (CVPR)*, pages 18973–18990, 2022.
 - [19] Madeleine Grunde-McLaughlin, Ranjay Krishna, and Maneesh Agrawala. Agqa: A benchmark for compositional spatio-temporal reasoning. In *2021 IEEE/CVF Conference on Computer Vision and Pattern Recognition (CVPR)*, pages 11282–11292, 2021.
 - [20] Kaiming He, Xiangyu Zhang, Shaoqing Ren, and Jian Sun. Deep residual learning for image recognition. In *2016 IEEE Conference on Computer Vision and Pattern Recognition (CVPR)*, pages 770–778, 2016.
 - [21] FC Heilbron, V Escorcia, B Ghanem, and J Niebles. A large-scale video benchmark for human activity understanding. In *Proceedings of the IEEE Conference on Computer Vision and Pattern Recognition, Boston, 2015. 961*, volume 970, 2019.
 - [22] Fabian Caba Heilbron, Victor Escorcia, Bernard Ghanem, and Juan Carlos Niebles. Activitynet: A large-scale video benchmark for human activity understanding. In *2015 IEEE*

- Conference on Computer Vision and Pattern Recognition (CVPR)*, pages 961–970, 2015.
- [23] Sepp Hochreiter and Jürgen Schmidhuber. Long short-term memory. *Neural computation*, 9(8):1735–1780, 1997.
 - [24] Jörg Hoffmann. The Metric-FF planning system: Translating “ignoring delete lists” to numeric state variables. *Journal of Artificial Intelligence Research*, 20:291–341, 2003.
 - [25] De-An Huang, Suraj Nair, Danfei Xu, Yuke Zhu, Animesh Garg, Li Fei-Fei, Silvio Savarese, and Juan Carlos Niebles. Neural task graphs: Generalizing to unseen tasks from a single video demonstration. In *Proceedings of the IEEE/CVF conference on computer vision and pattern recognition*, pages 8565–8574, 2019.
 - [26] Jingwei Ji, Ranjay Krishna, Li Fei-Fei, and Juan Carlos Niebles. Action genome: Actions as compositions of spatio-temporal scene graphs. In *Proceedings of the IEEE/CVF Conference on Computer Vision and Pattern Recognition*, pages 10236–10247, 2020.
 - [27] Baoxiong Jia, Ting Lei, Song-Chun Zhu, and Siyuan Huang. Egotaskqa: Understanding human tasks in egocentric videos. In *The 36th Conference on Neural Information Processing Systems (NeurIPS 2022) Track on Datasets and Benchmarks*, 2022.
 - [28] Yu-Gang Jiang, Jingen Liu, A Roshan Zamir, George Toderici, Ivan Laptev, Mubarak Shah, and Rahul Sukthankar. Thumos challenge: Action recognition with a large number of classes. <http://crcv.ucf.edu/THUMOS14/>, 2014.
 - [29] Diederik P Kingma and Jimmy Ba. Adam: A method for stochastic optimization. *arXiv preprint arXiv:1412.6980*, 2014.
 - [30] Eric Kolve, Roozbeh Mottaghi, Winson Han, Eli VanderBilt, Luca Weihs, Alvaro Herrasti, Daniel Gordon, Yuke Zhu, Abhinav Gupta, and Ali Farhadi. AI2-THOR: An Interactive 3D Environment for Visual AI. *arXiv*, 2017.
 - [31] Juho Lee, Yoonho Lee, Jungtaek Kim, Adam Kosior, Seungjin Choi, and Yee Whye Teh. Set transformer: A framework for attention-based permutation-invariant neural networks. In *International conference on machine learning*, pages 3744–3753. PMLR, 2019.
 - [32] Jie Lei, Licheng Yu, Mohit Bansal, and Tamara Berg. TVQA: Localized, compositional video question answering. In *Proceedings of the 2018 Conference on Empirical Methods in Natural Language Processing*, pages 1369–1379, Brussels, Belgium, Oct.-Nov. 2018. Association for Computational Linguistics.
 - [33] Junnan Li, Dongxu Li, Caiming Xiong, and Steven Hoi. Blip: Bootstrapping language-image pre-training for unified vision-language understanding and generation. In *International Conference on Machine Learning*, pages 12888–12900. PMLR, 2022.
 - [34] Jiangtong Li, Li Niu, and Liqing Zhang. From representation to reasoning: Towards both evidence and commonsense reasoning for video question-answering. In *Proceedings of the IEEE/CVF Conference on Computer Vision and Pattern Recognition (CVPR)*, June 2022.
 - [35] Linjie Li, Yen-Chun Chen, Yu Cheng, Zhe Gan, Licheng Yu, and Jingjing Liu. Hero: Hierarchical encoder for video+ language omni-representation pre-training. *arXiv preprint arXiv:2005.00200*, 2020.
 - [36] Liunian Harold Li, Pengchuan Zhang, Haotian Zhang, Jianwei Yang, Chunyuan Li, Yiwu Zhong, Lijuan Wang, Lu Yuan, Lei Zhang, Jenq-Neng Hwang, et al. Grounded language-image pre-training. In *Proceedings of the IEEE/CVF Conference on Computer Vision and Pattern Recognition*, pages 10965–10975, 2022.
 - [37] Yikang Li, Jenhao Hsiao, and Chiuman Ho. Videoclip: A cross-attention model for fast video-text retrieval task with image clip. In *Proceedings of the 2022 International Conference on Multimedia Retrieval*, pages 29–33, 2022.
 - [38] Xudong Lin, Fabio Petroni, Gedas Bertasius, Marcus Rohrbach, Shih-Fu Chang, and Lorenzo Torresani. Learning to recognize procedural activities with distant supervision. In *Proceedings of the IEEE/CVF Conference on Computer Vision and Pattern Recognition*, pages 13853–13863, 2022.
 - [39] J. Liu, Wenhui Chen, Yu Cheng, Zhe Gan, Licheng Yu, Yiming Yang, and Jingjing Liu. Violin: A large-scale dataset for video-and-language inference. *2020 IEEE/CVF Conference on Computer Vision and Pattern Recognition (CVPR)*, pages 10897–10907, 2020.
 - [40] Huaishao Luo, Lei Ji, Ming Zhong, Yang Chen, Wen Lei, Nan Duan, and Tianrui Li. Clip4clip: An empirical study of clip for end to end video clip retrieval and captioning. *Neurocomputing*, 508:293–304, 2022.
 - [41] Jiayuan Mao, Chuang Gan, Pushmeet Kohli, Joshua B. Tenenbaum, and Jiajun Wu. The Neuro-Symbolic Concept Learner: Interpreting Scenes, Words, and Sentences From Natural Supervision. In *International Conference on Learning Representations*, 2019.
 - [42] Weichao Mao, Ruta Desai, Michael Louis Iuzzolino, and Nitin Kamra. Action dynamics task graphs for learning plannable representations of procedural tasks. *arXiv preprint arXiv:2302.05330*, 2023.
 - [43] Antoine Miech, Jean-Baptiste Alayrac, Lucas Smaira, Ivan Laptev, Josef Sivic, and Andrew Zisserman. End-to-end learning of visual representations from uncurated instructional videos. In *Proceedings of the IEEE/CVF Conference on Computer Vision and Pattern Recognition*, pages 9879–9889, 2020.
 - [44] Tomas Mikolov, Kai Chen, Greg Corrado, and Jeffrey Dean. Efficient estimation of word representations in vector space. In *arXiv preprint arXiv:1301.3781*, 2013.
 - [45] OpenAI.
 - [46] Aishwarya Padmakumar, Jesse Thomason, Ayush Srivastava, Patrick Lange, Anjali Narayan-Chen, Spandana Gella, Robinson Piramuthu, Gokhan Tur, and Dilek Hakkani-Tur. Teach: Task-driven embodied agents that chat. In *Proceedings of the AAAI Conference on Artificial Intelligence*, volume 36, pages 2017–2025, 2022.
 - [47] Jeffrey Pennington, Richard Socher, and Christopher Manning. GloVe: Global vectors for word representation. In *Proceedings of the 2014 Conference on Empirical Methods in Natural Language Processing (EMNLP)*, pages 1532–1543, Doha, Qatar, Oct. 2014. Association for Computational Linguistics.

- [48] Yicheng Qian, Weixin Luo, Dongze Lian, Xu Tang, Peilin Zhao, and Shenghua Gao. Svip: Sequence verification for procedures in videos. In *Proceedings of the IEEE/CVF Conference on Computer Vision and Pattern Recognition*, pages 19890–19902, 2022.
- [49] Alec Radford, Jong Wook Kim, Chris Hallacy, Aditya Ramesh, Gabriel Goh, Sandhini Agarwal, Girish Sastry, Amanda Askell, Pamela Mishkin, Jack Clark, Gretchen Krueger, and Ilya Sutskever. Learning transferable visual models from natural language supervision. In Marina Meila and Tong Zhang, editors, *Proceedings of the 38th International Conference on Machine Learning*, volume 139 of *Proceedings of Machine Learning Research*, pages 8748–8763. PMLR, 18–24 Jul 2021.
- [50] Colin Raffel, Noam Shazeer, Adam Roberts, Katherine Lee, Sharan Narang, Michael Matena, Yanqi Zhou, Wei Li, and Peter J. Liu. Exploring the limits of transfer learning with a unified text-to-text transformer. *Journal of Machine Learning Research*, 21(140):1–67, 2020.
- [51] Michaela Regneri, Marcus Rohrbach, Dominikus Wetzel, Stefan Thater, Bernt Schiele, and Manfred Pinkal. Grounding action descriptions in videos. *Transactions of the Association for Computational Linguistics*, 1:25–36, 2013.
- [52] Keisuke Sakaguchi, Chandra Bhagavatula, Ronan Le Bras, Niket Tandon, Peter Clark, and Yejin Choi. proScript: Partially ordered scripts generation. In *Findings of the Association for Computational Linguistics: EMNLP 2021*, pages 2138–2149, Punta Cana, Dominican Republic, Nov. 2021. Association for Computational Linguistics.
- [53] Md. Kamruzzaman Sarker, Lu Zhou, Aaron Eberhart, and Pascal Hitzler. Neuro-symbolic artificial intelligence: Current trends. *CoRR*, abs/2105.05330, 2021.
- [54] Min Joon Seo, Aniruddha Kembhavi, Ali Farhadi, and Hananeh Hajishirzi. Bidirectional attention flow for machine comprehension. In *5th International Conference on Learning Representations, ICLR 2017, Toulon, France, April 24–26, 2017, Conference Track Proceedings*. OpenReview.net, 2017.
- [55] Yuhan Shen, Lu Wang, and Ehsan Elhamifar. Learning to segment actions from visual and language instructions via differentiable weak sequence alignment. In *Proceedings of the IEEE/CVF Conference on Computer Vision and Pattern Recognition*, pages 10156–10165, 2021.
- [56] Mohit Shridhar, Jesse Thomason, Daniel Gordon, Yonatan Bisk, Winson Han, Roozbeh Mottaghi, Luke Zettlemoyer, and Dieter Fox. ALFRED: A Benchmark for Interpreting Grounded Instructions for Everyday Tasks. In *The IEEE Conference on Computer Vision and Pattern Recognition (CVPR)*, 2020.
- [57] Gunnar A. Sigurdsson, Gül Varol, Xiaolong Wang, Ali Farhadi, Ivan Laptev, and Abhinav Gupta. Hollywood in homes: Crowdsourcing data collection for activity understanding. In Bastian Leibe, Jiri Matas, Nicu Sebe, and Max Welling, editors, *Computer Vision – ECCV 2016*, pages 510–526, Cham, 2016. Springer International Publishing.
- [58] Mattia Soldan, Alejandro Pardo, Juan León Alcázar, Fabian Caba Heilbron, Chen Zhao, Silvio Giancola, and Bernard Ghanem. Mad: A scalable dataset for language grounding in videos from movie audio descriptions. *arXiv preprint arXiv:2112.00431*, 2021.
- [59] Tomáš Souček, Jean-Baptiste Alayrac, Antoine Miech, Ivan Laptev, and Josef Sivic. Look for the change: Learning object states and state-modifying actions from untrimmed web videos. In *Proceedings of the IEEE Conference on Computer Vision and Pattern Recognition (CVPR)*, June 2022.
- [60] Sanjana Srivastava, Chengshu Li, Michael Lingelbach, Roberto Martín-Martín, Fei Xia, Kent Elliott Vainio, Zheng Lian, Cem Gokmen, Shyamal Buch, Karen Liu, Silvio Savarese, Hyowon Gwon, Jiajun Wu, and Li Fei-Fei. Behavior: Benchmark for everyday household activities in virtual, interactive, and ecological environments. In Aleksandra Faust, David Hsu, and Gerhard Neumann, editors, *Proceedings of the 5th Conference on Robot Learning*, volume 164 of *Proceedings of Machine Learning Research*, pages 477–490. PMLR, 08–11 Nov 2022.
- [61] Yansong Tang, Dajun Ding, Yongming Rao, Yu Zheng, Danyang Zhang, Lili Zhao, Jiwen Lu, and Jie Zhou. Coin: A large-scale dataset for comprehensive instructional video analysis. In *Proceedings of the IEEE/CVF Conference on Computer Vision and Pattern Recognition*, pages 1207–1216, 2019.
- [62] Makarand Tapaswi, Yukun Zhu, Rainer Stiefelhausen, Antonio Torralba, Raquel Urtasun, and Sanja Fidler. Movieqa: Understanding stories in movies through question-answering. In *2016 IEEE Conference on Computer Vision and Pattern Recognition (CVPR)*, pages 4631–4640, 2016.
- [63] Tristan Thrush, Ryan Jiang, Max Bartolo, Amanpreet Singh, Adina Williams, Douwe Kiela, and Candace Ross. Winoground: Probing vision and language models for visiolinguistic compositionality. In *Proceedings of the IEEE/CVF Conference on Computer Vision and Pattern Recognition*, pages 5238–5248, 2022.
- [64] Dorin Ungureanu, Federica Bogo, Silvano Galliani, Pooja Sama, Xin Duan, Casey Meekhof, Jan Stühmer, Thomas J Cashman, Bugra Tekin, Johannes L Schönberger, et al. Hololens 2 research mode as a tool for computer vision research. *arXiv preprint arXiv:2008.11239*, 2020.
- [65] Jason Wei, Xuezhi Wang, Dale Schuurmans, Maarten Bosma, brian ichter, Fei Xia, Ed H. Chi, Quoc V Le, and Denny Zhou. Chain of thought prompting elicits reasoning in large language models. In Alice H. Oh, Alekh Agarwal, Danielle Belgrave, and Kyunghyun Cho, editors, *Advances in Neural Information Processing Systems*, 2022.
- [66] Laurence A Wolsey. *Integer programming*. John Wiley & Sons, 2020.
- [67] Bo Wu, Shoubin Yu, Zhenfang Chen, Joshua B Tenenbaum, and Chuang Gan. Star: A benchmark for situated reasoning in real-world videos. In *Thirty-fifth Conference on Neural Information Processing Systems (NeurIPS)*, 2021.
- [68] Junbin Xiao, Xindi Shang, Angela Yao, and Tat-Seng Chua. Next-qa: Next phase of question-answering to explaining temporal actions. In *Proceedings of the IEEE/CVF Conference on Computer Vision and Pattern Recognition (CVPR)*, pages 9777–9786, June 2021.

- [69] Ning Xie, Farley Lai, Derek Doran, and Asim Kadav. Visual entailment: A novel task for fine-grained image understanding. *arXiv preprint arXiv:1901.06706*, 2019.
- [70] Saining Xie, Chen Sun, Jonathan Huang, Zhuowen Tu, and Kevin Murphy. Rethinking spatiotemporal feature learning: Speed-accuracy trade-offs in video classification. In Vittorio Ferrari, Martial Hebert, Cristian Sminchisescu, and Yair Weiss, editors, *Computer Vision – ECCV 2018*, pages 318–335, Cham, 2018. Springer International Publishing.
- [71] Yaqi Xie, Chen Yu, Tongyao Zhu, Jinbin Bai, Ze Gong, and Harold Soh. Translating natural language to planning goals with large-language models. *arXiv preprint arXiv:2302.05128*, 2023.
- [72] Haosen Yang, Wenhao Wu, Lining Wang, Sheng Jin, Boyang Xia, Hongxun Yao, and Hujie Huang. Temporal action proposal generation with background constraint. In *Proceedings of the AAAI conference on artificial intelligence*, volume 36, pages 3054–3062, 2022.
- [73] Kexin Yi, Chuang Gan, Yunzhu Li, Pushmeet Kohli, Jiajun Wu, Antonio Torralba, and Joshua B. Tenenbaum. CLEVRER: collision events for video representation and reasoning. In *8th International Conference on Learning Representations, ICLR 2020, Addis Ababa, Ethiopia, April 26-30, 2020*. OpenReview.net, 2020.
- [74] Kexin Yi, Jiajun Wu, Chuang Gan, Antonio Torralba, Pushmeet Kohli, and Joshua B. Tenenbaum. Neural-symbolic vqa: Disentangling reasoning from vision and language understanding. In *Proceedings of the 32nd International Conference on Neural Information Processing Systems, NIPS’18*, page 1039–1050, Red Hook, NY, USA, 2018. Curran Associates Inc.
- [75] Jiahui Yu, Zirui Wang, Vijay Vasudevan, Legg Yeung, Mojtaba Seyedhosseini, and Yonghui Wu. Coca: Contrastive captioners are image-text foundation models. *Transactions on Machine Learning Research*, 2022.
- [76] Mert Yuksekgonul, Federico Bianchi, Pratyusha Kalluri, Dan Jurafsky, and James Zou. When and why vision-language models behave like bags-of-words, and what to do about it? In *International Conference on Learning Representations*, 2023.
- [77] Amir Zadeh, Michael Chan, Paul Pu Liang, Edmund Tong, and Louis-Philippe Morency. Social-iq: A question answering benchmark for artificial social intelligence. In *2019 IEEE/CVF Conference on Computer Vision and Pattern Recognition (CVPR)*, pages 8799–8809, 2019.
- [78] Andy Zeng, Maria Attarian, brian ichter, Krzysztof Marcin Choromanski, Adrian Wong, Stefan Welker, Federico Tombari, Aveek Purohit, Michael S Ryoo, Vikas Sindhwani, Johnny Lee, Vincent Vanhoucke, and Pete Florence. Socratic models: Composing zero-shot multimodal reasoning with language. In *International Conference on Learning Representations*, 2023.
- [79] Yiwu Zhong, Jianwei Yang, Pengchuan Zhang, Chunyuan Li, Noel Codella, Liunian Harold Li, Luwei Zhou, Xiyang Dai, Lu Yuan, Yin Li, et al. Regionclip: Region-based language-image pretraining. In *Proceedings of the IEEE/CVF Conference on Computer Vision and Pattern Recognition*, pages 16793–16803, 2022.
- [80] Liu Zhuang, Lin Wayne, Shi Ya, and Zhao Jun. A robustly optimized BERT pre-training approach with post-training. In *Proceedings of the 20th Chinese National Conference on Computational Linguistics*, pages 1218–1227, Huhhot, China, Aug. 2021. Chinese Information Processing Society of China.
- [81] Dimitri Zhukov, Jean-Baptiste Alayrac, Ramazan Gokberk Cinbis, David Fouhey, Ivan Laptev, and Josef Sivic. Cross-task weakly supervised learning from instructional videos. In *2019 IEEE/CVF Conference on Computer Vision and Pattern Recognition (CVPR)*, pages 3532–3540, 2019.

Appendix for “EgoTV : Egocentric Task Verification from Natural Language Task Descriptions”

This appendix is organized as follows:

7. *EgoTV dataset*: Details on generation process, additional statistics.
8. *CrossTask Verification (CTV) dataset*: Details on generation process and evaluation.
9. *NSG*: Semantic parsing approaches, additional analysis and ablations, performance on CTV.
10. *Baselines*: Details on VLM and Oracle baselines.

We will release the code and dataset upon acceptance. A few sample videos & annotations from the EgoTV dataset are provided in [EgoTV data/](#) in the supplementary material. We also include demo videos showing how NSG works on the dataset in the folder [DemoVideo/](#). Lastly, the code for generating the dataset as well as for NSG and the baselines is in the folder [Code/](#).

7. EgoTV Dataset

7.1. Task-video Generation using PDDL Planner

To generate EgoTV tasks, we encode the final state of the objects achieved by an EgoTV task as the “goal state” for the Planning Domain Definition Language (PDDL) planner. Note that the ordering constraints of the tasks aren’t captured when the tasks are encoded as goal states for the PDDL planner in this manner. For instance, the tasks of *clean_then_heat(apple)* and *clean_and_heat(apple)* would have the same PDDL goal states. Consequently, we enforce ordering constraints for a given task using “pre-conditions” in PDDL. In the above example task of *clean_then_heat(apple)*, the *clean* sub-task would thus be the pre-condition for the *heat* sub-task. Apart from the tasks and object states, the agent state and environment dynamics – e.g., the *heat* sub-task changes the state of the target object to be hot – are also encoded in PDDL.

For each task, a random kitchen scene is picked and the agent is spawned in the corresponding AI2-THOR scene. The planner leverages the initial state and action definitions to generate a sequence of sub-tasks required to achieve the goal state. Rather than simply selecting the best plan, which may not always reflect human-like behavior, we aim to mimic the less-than-optimal decision-making of humans by randomly selecting a plan from the top- k plans. This approach enables the inclusion of sub-tasks that may not be strictly necessary for achieving the ultimate goal. Furthermore, the partial-ordered nature of tasks enables different

plan generations to achieve the same task, thus promoting diversity in the dataset. We use the Fast Forward (FF) planner [24] to generate plans.

Apart from sequencing the sub-tasks appropriately for achieving a given task, the planner also ensures that the agent can navigate to the correct locations for each sub-task. For instance, to execute the *clean* sub-task, an agent typically requires using the sink in the kitchen and hence must navigate there. The generated plans thus consist of navigation and object interaction actions.

7.2. EgoTV Task-description Generation

The task descriptions corresponding to negative samples, where the task videos are not entailed by their descriptions, are created by either altering the sequence of sub-tasks in the positive template or by replacing some of them with alternative sub-tasks picked randomly from the remaining repertoire of sub-tasks (see Figure 1 where *heat* is replaced with *cool*). To ensure the practicality of an assistive agent that aids a human, we maintain the target object in the negative samples but vary the sub-tasks, as negative task descriptions on the sub-task level are more relevant than on the object level. For abstraction we (i) omit the low-level details like *clean in the sinkbasin*, *cool in the fridge*; (ii) (some) task-oriented descriptions are changed to goal-oriented descriptions (*apple is heated and cleaned* \mapsto *hot, clean apple*).

An example template of task descriptions corresponding to the task *cool_then_clean* is [$\{obj\}$ is cooled in a Fridge, then cleaned in a SinkBasin], [$\{obj\}$ is cleaned in a SinkBasin after cooling in a Fridge], [$\{obj\}$ is cooled in a Fridge before cleaning in a SinkBasin]

7.3. Dataset Analysis and Statistics

See Figure 5 for a comparison of video lengths and task description lengths across different splits. It can be observed that the Novel Tasks split has the longest videos (≈ 1.6 minutes) and task descriptions (≈ 12 words) owing to its compositional tasks. Additionally, the Abstraction split has the shortest task description (≈ 5 words), even for longer videos due to abstraction. We include all tasks of EgoTV in Table 9 at the end of the supplement.

	Reasoning		Dataset Characteristics				Grounding	
	compositional	causal	language	egocentric	real-world	diagnostic tools	objects, relations	actions
CLEVRER [73]	✓	✓	✓	✗	✗	✓	✓	✗
Next-QA [68]	✗	✓	✓	✗	✓	✓	✓	✓
AGQA [19]	✓	✗	✓	✗	✓	✓	✓	✓
Activity	✗	✗	✓	✗	✓	✗	✓	✓
Net-QA [22]	✗	✗	✓	✗	✓	✗	✓	✓
STAR [67]	✓	✓	✓	✗	✓	✓	✓	✓
CoPhy [7]	✗	✓	✗	✗	✗	✓	✓	✗
Social-IQ [77]	✗	✓	✓	✗	✓	✓	✗	✗
Causal-VidQA [34]	✗	✓	✓	✗	✓	✓	✓	✓
Charades [57]	✗	✗	✓	✗	✓	✓	✓	✓
CATER [17]	✓	✗	✗	✗	✗	✓	✓	✓
EPIC-KITCHENS [12]	✓	✓	✓	✓	✓	✓	✓	✓
Ego-4D [18]	✗	✓	✓	✓	✓	✓	✓	✓
VIOLIN [39]	✗	✓	✓	✗	✓	✗	✓	✓
Change-It [59]	✗	✓	✗	✓	✓	✗	✓	✓
Cross-Task [81]	✓	✗	✓	✗	✓	✗	✓	✓
EgoTV 📺	✓	✓	✓	✓	✗	✓	✓	✓

Table 4. **EgoTV vs. existing video-language datasets.** EgoTV benchmark enables reasoning (compositional, causal, and temporal); has unique dataset characteristics along with capabilities for systematic investigation (diagnostics); requires grounding of objects, relations, and actions.

Topics	Tasks
Make beverage	Make Jello Shots, Make a Latte, Make Lemonade, Make Irish Coffee
Make food	Make Taco Salad, Grill Steak, Make Kimchi Fried Rice, Make Meringue, Make Kerala Fish Curry, Make Butter Pickles
Make dessert	Make French Toast, Make Banana Ice Cream, Make French Strawberry Cake, Make Pancakes
Fix car	Jack Up a Car, Add Oil to Your Car, Change a Tire

Table 5. **Task Topics in CTV.** Each task with a shared task topic contains shared action steps.

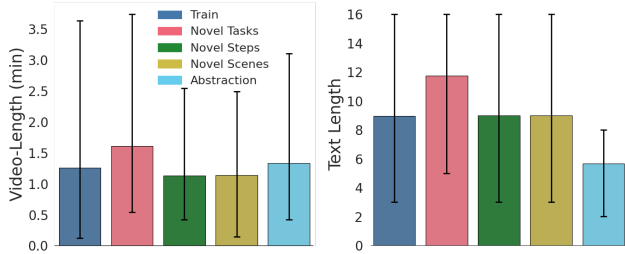


Figure 5. **Additional EgoTV dataset statistics.** Comparison of video length (in minutes) and task description length (number of words) across different splits using error plots. Novel Tasks split has the longest videos and task descriptions. Abstraction split has the shortest task descriptions.

8. CrossTask Verification (CTV) Dataset

8.1. Problem setting

Taking inspiration from our proposed EgoTV dataset, we construct a new dataset CrossTask Verification from CrossTask dataset [81] to test the model’s performance on real-world videos. CrossTask [81] has 18 task classes with around 150 videos per class. Given each task, e.g., *fixing tire*, there are corresponding action steps, *jack up*, *change tire* to accomplish such task. Also, the action steps across

different tasks are possibly shared, e.g., *add sugar* in *Make lemonade* or *Make coffee*. The temporal annotation of each action step is available. In CrossTask Verification evaluation, given a task description and the video, the model needs to predict if the task is accomplished (entailed) in the video. Akin to EgoTV, CTV consists of paired task descriptions and videos for task verification. We construct two settings:

- Action sequence verification** NL descriptions are obtained by leveraging action step annotations in CrossTask.
- Task verification** task class-labels are used as descriptions.

In the first setting, the model needs to understand if the action steps were executed successfully in order. Since the action steps are usually short-term actions with only a few seconds, the model needs to localize the correct action step temporal location with finer granularity. In the second setting, the task class was given instead of the action step level. The model needs to understand the task as a whole (consisting of several action steps to accomplish), and a more global understanding is required.

8.2. Dataset construction

We leverage the CrossTask dataset and its action step annotation to construct our CrossTask Verification dataset

Query Type	Signature	Semantics
StateQuery	(Object, State), Video $\mapsto \mathbb{P}$	Queries the state (<i>hot, cold, clean, ripe</i>) of object in a video and returns the probability of the object state being detected. Example instructions: <i>heat an apple, clean a spoon.</i>
RelationQuery	(Object, Object/Receptacle, Relation), Video $\mapsto \mathbb{P}$	Queries the relation between two objects or an object and a receptacle in a video and returns the probability of the relation being detected. Example instructions: <i>put apple in basket, place spoon to the left of plate.</i>
ActionQuery	(Subtask, *Objects, *Relation), Video $\mapsto \mathbb{P}$	Queries for a sub-task with one or more arguments (*) in a video and returns the probability of the sub-task being executed. Example instructions: <i>whisk mixture, pour lemonade into glass.</i>

Table 6. NSG’s query types for task verification in EgoTV and CTV. The query types `StateQuery` and `RelationQuery` are used in EgoTV, whereas `ActionQuery` is used in CrossTask. Each query type τ is modeled using a neural network f^{θ_τ} accepts unique arguments (a) and video frames (v) as input and generates an output probability $\mathbb{P} = f^{\theta_\tau}(a, v)$ of the query being true in the video v .

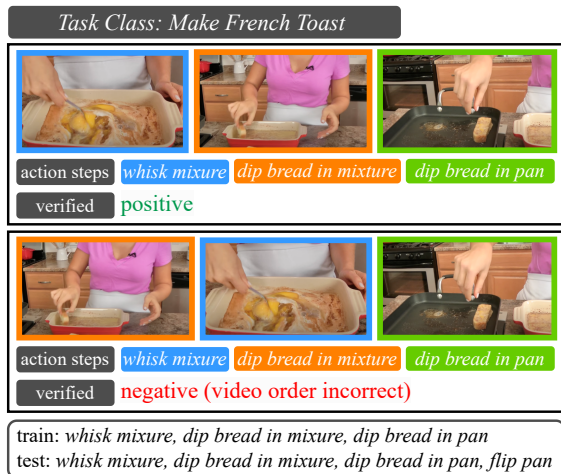


Figure 6. CrossTask Verification (CTV) dataset.

with the following two splits:

(1) **Action sequence verification** is done by concatenating a sequence of *action steps* annotated in CrossTask for each video as our task description.

- To ensure repetitive subtasks, as in EgoTV, we start by selecting the action steps within each task based on frequency. In the end, we select the 4 most frequent action steps with respect to each task. We then filter out video segments in CrossTask that don’t contain the top 4 frequent action steps.
- We also followed a similar process of EgoTV for generating negative descriptions. We include three ways of **negative description** including: (i) *replacing action steps from other tasks*: where we substitute one of the action steps in the sequence to the action step in another task. (ii) *replacing action steps from the same task*: instead of replacing step from another task, we reuse the unused action steps which were not the top 4 frequent steps in the same task. These action steps are closer in semantics and serve as hard negative. (iii) *replace action step sequence order to impossible sequence*: we first list out all possible action step orders in CrossTask following [42]. Then, we

found an action sequence that doesn’t exist in CrossTask, e.g., *lower jack, upper jack, break on*. We called these sequence orders impossible since we can’t lower the jack when the car is already on the ground. To make the task more challenging, we also generate **negative videos** by (i) *shuffling the video order corresponding to each action step*: where the action steps weren’t executed in the correct order. (ii) *dropping a video segment corresponding to its action step*: where one action step is missing in the video. Therefore, the task wasn’t executed successfully.

(2) **Task verification** is a more challenging setting where we directly use the **task class** of the video as the task description. Instead of generating negative samples as in *action sequence verification*, the negative samples are from different task classes. We select a negative task class with shared action steps to ensure the model understands the procedure of a certain task instead of simply object-level recognition. We divide the task classes into 4 major topics as shown in Table 5, where each topic contains shared action steps as described in Section 8.1. The video follows the same process as *Action sequence verification* where we select videos with the top 4 action steps.

8.3. Evaluation

Metrics. We follow EgoTV to use accuracy and F1 to measure the efficacy of models on CrossTask Verification benchmark. We also evaluate model scalability by testing on tasks with varying complexity and ordering.

Generalization. In *Action sequence verification*, we construct a test set using videos with unseen action compositions. While this is equivalent to Novel Task split (Sec. 3.2.2) from EgoTV in spirit, CTV test set also contains some amount of novel visual context and steps due to limited control during generation. To ensure that our split has novel sub-tasks, we train with videos with maximum 3 sub-tasks/steps and test with videos containing 4 sub-tasks as shown in Figure 6. Note that all action steps which exist in testing also exist in training to ensure all steps were observed.

Table 8.3: Semantic Parsing by Prompting ChatGPT

Q. slice of apple is heated in microwave, then placed in a plate
A. First the apple is sliced, hence Step 1: slice apple. Then the apple is heated, hence Step 2: heat apple. Then the apple is placed in a plate, hence Step 3: place apple in plate. Hence, the order of the steps are: slice apple < heat apple < place apple in plate

Q. potato is cleaned in sinkbasin and sliced, then cooled in a fridge
A. First the potato is cleaned and sliced in any order, hence Step 1: clean potato; Step 2: slice potato. Then the potato is cooled in a Fridge, hence Step 3: cool potato. Hence, the order of the steps are: clean potato and slice potato < cool potato

Q. hot, sliced, clean tomato
A. First the tomato is heated and sliced and cleaned in any order, hence Step 1: heat tomato; Step 2: slice tomato; Step 3: clean tomato. Hence, the order of the steps are: heat tomato and slice tomato and clean tomato

Q. apple is heated and cleaned in sinkbasin, then cooled and sliced
A. First the apple is heated and cleaned in a sink basin in any order, hence Step 1: heat apple; Step 2: clean apple. Then the apple is cooled and sliced in any order, hence Step 3: cool apple; Step 4: slice apple. Hence, the order of the steps are: heat apple and clean apple < cool apple and slice apple.

Q. sliced apple is heated in microwave, then cleaned in a sinkbasin
A. First the apple is sliced, hence Step 1: slice apple. Then the apple is heated in a microwave, hence Step 2: heat apple. Then the apple is cleaned in a sink basin, hence Step 3: clean apple. Hence, the order of the steps are: slice apple < heat apple < clean apple

Q. apple is heated in microwave after cooling and cleaning
First the apple is cooled and cleaned in any order, hence Step 1: cool apple; Step 2: clean apple. Then the apple is heated in a microwave, hence Step 3: heat apple. Hence, the order of the steps are: cool apple and clean apple < heat apple.

9. NSG details

The query types used by NSG for both the EgoTV dataset and the CTV dataset are shown in Table 6.

9.1. NSG code

We include our NSG code in the folder [Code/nsg](#) comprising the training code for (State+Relation)Query model in *nesy.v1.py* and ActionQuery model in *nesy.v2.py*.

9.2. NSG Training details

When training NSG, we do not update the weights of the CLIP feature extractors (Sec. 4.3) due to GPU memory limitations. We use a batch of $N = 64$ samples, where we sample the video at 2.5 FPS. We set a window size $k = 20$ frames for segmentation in NSG (Sec. 4.4), each window representing an 8-second video segment. We use a train-validation split of 80-20 and use the validation performance as an indicator of convergence. We minimize the binary

cross-entropy loss in Eq. 2 with Adam [29] and a learning rate of $1e-3$. Each model is trained on 8 V100 GPUs for 50 epochs for two days.

9.3. NSG Semantic Parsing

We test two semantic parsing methods: (i) Finetuning language models to generate graphs from NL descriptions; (ii) Few-shot prompting of large language models.

9.3.1 Finetuning Language Models

Recently, it has been shown that pre-trained language models can be leveraged for graph [52] and plan generation [71] from NL. We use a similar framework to train a T5-small transformer [50] to generate partial-ordered plans. For this, we use a subset of the training data (in particular the positive task descriptions for which we have gold-label graphs annotations) and annotate them with their partial-ordered plans in the form of directed acyclic graphs (DAG) – $G(V, E)$, where vertices $n_i \in V$

represent sub-tasks, and edges $e_{ij} \in E$ are ordering constraints that indicate n_i must precede n_j (i.e. $n_i \rightarrow n_j$). To train the text generation transformer, we represent the output graph in DOT language. The corresponding DOT representation for the graph in Figure 3 is given as: Step 0: StateQuery(apple, hot), Step 1: StateQuery(apple, clean), Step 2: StateQuery(apple, sliced), Step 3: RelationQuery(apple, plate, in), Step 0 \rightarrow Step 1, Step 0 \rightarrow Step 2, Step 1 \rightarrow Step 3, Step 2 \rightarrow Step 3

Ablations on Plan Generation framework: We assess the correctness of the graphs generated by the trained T5-transformer model on the positive task descriptions of our test splits. The evaluation metric is Graph Edit Distance (GED) [3] which computes the distance between two graphs (G_1 and G_2) given as:

$$GED(G_1, G_2) = \min_{G_1 \xrightarrow{d_1, \dots, d_k} G_2} \sum_{i=1}^k cost(d_i)$$

where, d_1, \dots, d_k are graph edit operations (insertion, deletion, replacement of a vertex or an edge) from G_1 to G_2 . With the exception of the abstraction split⁶, the GED for all test splits was observed to be ≈ 0.03 (GED \downarrow). Here, \downarrow signifies that a lower GED score is better, with the lowest value being = 0. Note, that although it is possible for the response to contain syntax errors, e.g., invalid names or queries with invalid arguments, the output can be improved by leveraging the DSL grammar to avoid invalid arguments.

9.3.2 Prompting Language Models

We also experimented with prompting. As a proof-of-concept, we show our example prompts in Table 8.3. We use ChatGPT [45] with few-shot prompting. The prompt is displayed in gray, the queries in blue, and the generated output in green. We observed that the use of Chain-of-Thought [65] improved the output.

9.4. Integer Programming for Alignment in NSG

The constrained optimization problem defined in Eqs. 3, without the ordering constraint, can also be formulated as an Integer Programming problem [66] where variables Z_{jt} can only take integer values in $\{0, 1\}$ (i.e. with the additional constraint $Z \in \{0, 1\}^{N \times S}$).

⁶For abstraction, we observed syntax errors, e.g., missing/incorrect arguments for queries in the generated graphs like `RelationQuery(apple, slice)`, instead of `RelationQuery(apple, knife, slice)`. However, the selection of the correct query module and the partial grounding of the correct arguments lead to a significant improvement over baselines.

NSG	Novel Tasks	Novel Steps	Novel Scenes	Abstraction
$k = 12$	90.6	50.3	81.3	82.5
$k = 20$ (default)	90.0	64.7	84.9	80.4
$k = 32$	89.2	54.9	81.0	82.3
NSG-BiLSTM	73.3	70.2	90.0	87.2

Table 7. **NSG ablations.** [Block 1]: NSG with different window sizes $k = \{12, 20, 32\}$. The best-performing NSG model with $k = 20$ is reported in Table 2. [Block 2]: NSG with BiLSTM to encode additional context from neighboring segments.

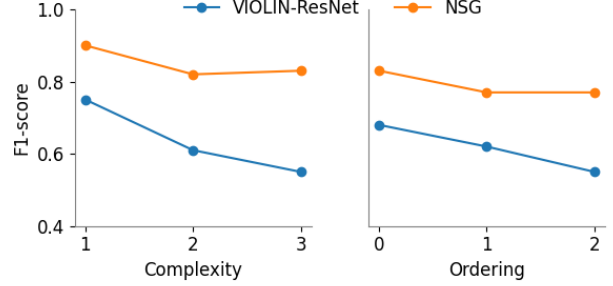


Figure 7. **NSG maintains consistent performance as task complexity and ordering difficulty increases.** F1-score of NSG vs. best-performing baseline for EgoTV tasks with varying complexity and ordering are shown.

It is important to note that the proposed DP solution adheres to the constraints Eqs. 3a 3b3c. The first part of the DP (highlighted in green in Figure 3) pairs the current query s_j with the current segment s_t , then tries to align the rest of the queries with the remaining segments to meet the requirement of one query per segment, as specified in Eq. 3a. The second part of the solution (denoted by the red box) skips over the current segment s_t and tries to align the same queries with the remaining segments until a pairing is found (i.e. $Z_{jt} = 1$). Thus, together with the base case of $Z = \mathbb{I}$ if $N = S$, it satisfies Eq. 3b. Furthermore, since the DP processes the queries and segments in a specific order (topological sorting for queries and temporal order of video segments), it also meets the ordering constraint requirement specified in Eq. 3c.

9.5. NSG Analysis

- Table 7 demonstrates the robustness of NSG to changes in the window size k . Specifically, we observe that NSG’s performance is minimally affected by varying the window size parameter.
- We trained two different NSG models to compare the impact of query types: one with `StateQuery` and `RelationQuery`, and another with `ActionQuery`. Figure 8 reveals that a combination of `(State+Relation)Query` is effective at detecting sub-tasks in segments with high recall,

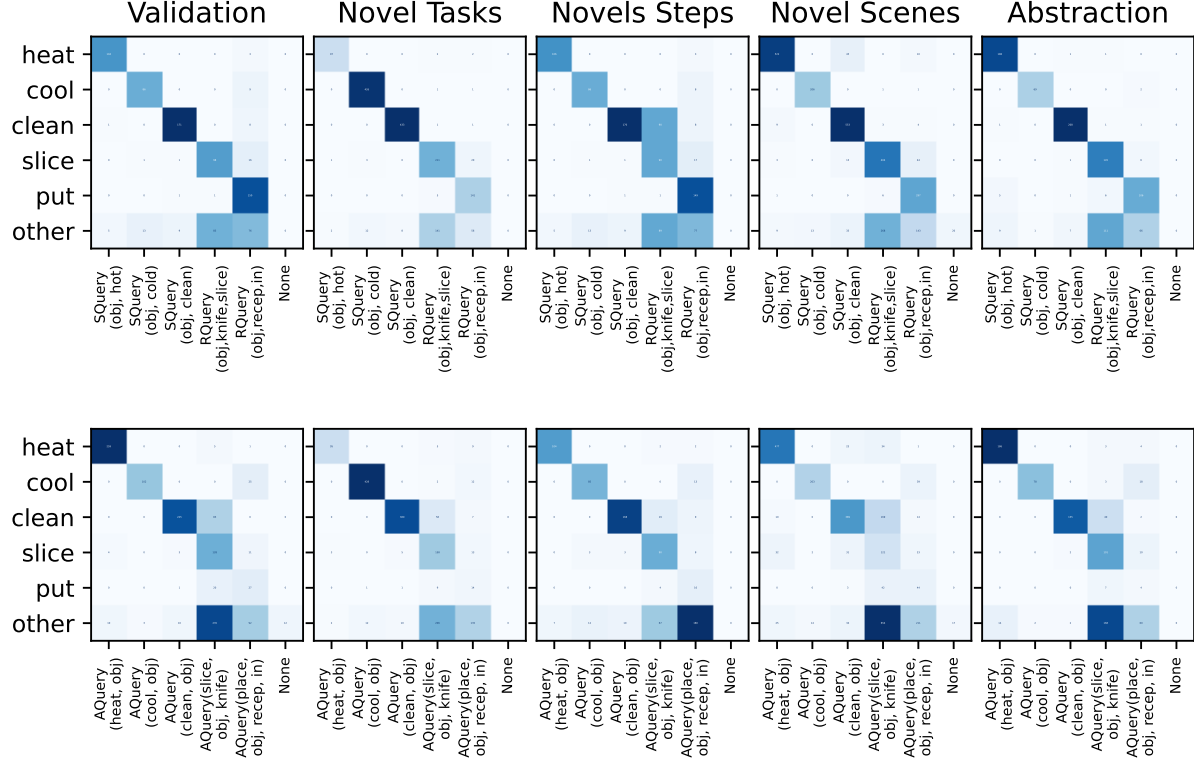


Figure 8. **Effect of query types on NSG performance.** Confusion matrices for two different query models across train/test splits of EgoTV. The Y-axis represents the ground-truth sub-task for a segment, and the X-axis denotes the aligned query for that segment. [Row 1]: Here, SQuery and RQuery denote *StateQuery* & *RelationQuery*, respectively. [Row 2]: Here, AQuery denotes *ActionQuery*. It can be observed that $\{\text{State+Relation}\}\text{Query}$ performs better than *ActionQuery*.

particularly for sub-tasks like *slice* and *put*. We also note that the NSG model struggles to detect the *slice* sub-task in the Novel Steps split.

- We evaluated the NSG model against the best-performing baseline (VIOLIN-ResNet) across two axes: task complexity and ordering. Figure 7 shows that NSG’s performance is robust to complexity and ordering variations.
- Since NSG only utilizes the features from aligned video segments and ignores the remaining segments, we conducted experiments to investigate the role of context (from the discarded segments) in EgoTV task verification. Specifically, we trained an extra BiLSTM layer to encode bidirectional context from adjacent segments on top of the CLIP-based segment features. As depicted in Table 7, we observed improved performance across all splits, except for Novel Tasks. We attribute this reduction in performance to a potential loss of compositional and temporal comprehension of the segment features caused by the inclusion of additional context information.

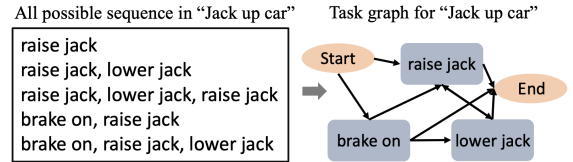


Figure 9. **CrossTask Verification (CTV) Graph construction.**

Model	Task description	F1
VIOLIN-I3D [39]	Action label	34.7
MIL-NCE [43]	Action label	43.4
VideoCLIP [37]	Action label	49.7
CoCa [75]	Action label	70.9
NSG (ours)	Action label	76.3
VIOLIN-I3D [39]	Task class	32.5
MIL-NCE [43]	Task class	40.1
VideoCLIP [37]	Task class	43.5
CoCa [75]	Task class	65.3
NSG (ours)	Task class	71.4

Table 8. **Performance on CTV’s Novel Tasks split**

Table 9.5: Text2Text Baseline Examples

Text Description

apple is cooled in a Fridge and cleaned in a SinkBasin

Video Caption

Segment: 1. Location: kitchen. Objects: countertop, apple. Activity: go to countertop
 Segment: 2. Location: kitchen. Objects: fridge, apple. Activity: go to fridge
 Segment: 3. Location: kitchen. Objects: apple, fridge. Activity: cool apple
 Segment: 4. Location: kitchen. Objects: apple, fridge. Activity: cool apple
 Segment: 5. Location: kitchen. Objects: sink, apple. Activity: go to sink
 Segment: 6. Location: kitchen. Objects: apple, sink. Activity: clean apple

Task Verified

True

Text Description

lettuce is picked, cooled in a Fridge, and sliced in a SinkBasin

Video Caption

Segment: 1. Location: kitchen. Objects: sink,lettuce. Activity: go to sink
 Segment: 2. Location: kitchen. Objects: sink,lettuce. Activity: go to sink
 Segment: 3. Location: kitchen. Objects: lettuce, sink. Activity: clean lettuce
 Segment: 4. Location: kitchen. Objects: fridge, lettuce. Activity: go to fridge
 Segment: 5. Location: kitchen. Objects: lettuce, fridge. Activity: cool lettuce

Task Verified

False

9.6. NSG on Real-world Data

NSG for CTV. In Section 4.1, we described two symbolic operations to process task description. In CTV, all of the action steps refer to a certain action. Hence, we apply the `ActionQuery` as in Table 6 to encode all action steps. In Section 4.2, we described (1) how we processed task description into a graph and (2) how we generated all possible sequences from the graph. In our *action sequence verification* setting, the ground truth action sequence was given as the task description. Hence, we directly feed the sequence in our later model Query Encoders and Video Aligner. In our *task verification* setting, only the task class was given. Here, instead of generating a graph from the task description, we follow [42] to construct a graph given each task by all possible sequence order as shown in Figure 9. Then, we feed the graph to the rest of our model.

Performance Evaluation. To evaluate how NSG enables task verification in the real world, we compare the performance of NSG against selected baselines described in Sec. 5, which were either applied to the previous CrossTask evaluation (MIL-NCE[43], VideoCLIP[37]) or had competitive performance (CoCa[75], VIOLIN[39]) on EgoTV. Note that the methods for CrossTask are not directly applicable to CTV since CTV focuses on task verification (predicting if the task is accomplished) instead of temporal localization(localizing action temporally). Table 8 shows that the baseline models VideoCLIP, CoCa perform better than VIOLIN on CTV as compared to EgoTV. This indicates

that CTV is potentially able to better harness the gains from the large-scale VL pretraining in these models compared to EgoTV. Despite these gains, NSG outperforms the baselines by a significant margin in both action sequence and task verification settings. We also found the *Task verification* setting is more challenging than *Action sequence verification* setting in general since the former offers much less information for the model to predict. Also, the same task may have different ways to accomplish it. The model needs to learn such diverse steps inherently. The results demonstrate the applicability of NSG’s causal and compositional reasoning capabilities in the real world.

10. Baseline descriptions and details

10.1. VLM Baselines

Majority of VLMs can be characterized based on their approach of extracting and fusing features from vision and text modalities. VLMs for video tasks use either a video encoder or an image encoder with temporal aggregation using sequence model, e.g., transformers [50] or LSTM [23] to obtain the video features. The vision and text encoders can be jointly trained using either a) contrastive loss that aligns both modalities in a shared latent space e.g., CLIP [49], MIL-NCE [43], b) masked token prediction losses on the generated text [33] aka captioning loss, or c) combination of captioning and contrastive losses [75]. The vision-text features from encoders can either be fused (multimodal fusion) using attention-based mechanisms or by computing cross-modal similarity scores. We investigate 6 VLMs that

CLIP4Clip [40] uses CLIP-based [49] text and image encoders. Parameterized (e.g., LSTM-based) or non-parameterized (e.g., mean-pooling) aggregation of the resultant image features allows video representation using a single feature vector, without any explicit fusion. **CLIP Hitchhiker [5]** uses a similar encoder structure as CLIP4Clip [40] and performs weighted-mean pooling of frame embeddings using text-visual similarity scores. **CoCa [75]** uses image-text (dual) encoder-decoder architecture trained using contrastive and captioning loss. The frame-level features are pooled via attentional pooling [31] to model the temporal sequence of the video and then fused with the text features for downstream tasks. **MIL-NCE [43]** learns to encode video and text into a single vector using separate encoders (S3D[70], word2vec[44]) learned from scratch using the proposed multi-instance contrastive loss. **VideoCLIP [37]** is built on top of MIL-NCE [43]. It adds additional transformer layers for video and text encoders, trained using contrastive loss. The resultant embeddings can be fused together for downstream tasks. **VIOLIN [39]** uses pre-trained image/video (e.g., ResNet [20], I3D [9]) and text encoders (e.g., GloVe [47], BERT [13]) separately and fuses the resultant representations from each modality using bi-directional attention [54]. For each of the above VLMs, we freeze the pretrained feature extractors for each modality and finetune a fully-connected probe layer, along with the temporal aggregation layers where appropriate (CLIP4Clip-LSTM, VIOLIN), using EgoTV’s train split.

In this baseline, we generate video captions from ground-truth objects and sub-task labels and calculate a text similarity score (cosine similarity) between the video caption and the task description using a pretrained RoBERTa model [80] by using a manually set threshold. We start by splitting the video into segments and generate captions for each segment comprising the segment index (for temporal grounding), scene location (kitchen), (*top-k*) objects in the scene, and the activity (sub-task). Example tasks are shown in Table 9.5. This baseline is analogous to Socratic Models [78] which generalizes to new applications in zero-shot by leveraging the multimodal capabilities from several pre-trained models. For instance, the objects from each segment can be captured using open-vocabulary VLMs [36, 79, 75], while the activities for each segment can be detected using [43, 37] by zero-shot classification with text-to-video feature similarity. Similarly, a final summarized video caption for the whole video can be generated using an LLM.

model has limited capacity to capture (out-of-domain) word-level sub-task orderings to determine entailment in EgoTV, and (2) Text2Text lacks visual inputs and might suffer from lack of inferring relationships between objects like those captured by `RelationQuery` types.

Table 9. **List of tasks in EgoTV dataset** arranged according to complexity (rows) and ordering (columns) in the tasks. A total of 82 tasks were considered for the dataset generation, split into train and sub-goal composition sets. **Blue** is used to denote the tasks in sub-goal composition split.